Solar Energy 181 (2019) 357–360

Contents lists available at ScienceDirect

Solar Energy

journal homepage: www.elsevier.com/locate/solener

Germanium photovoltaic cells with MoO_x hole-selective contacts

A. Alcañiz[a], G. López[a], I. Martín[a,*], A. Jiménez[b], A. Datas[a,b,*], E. Calle[a], E. Ros[a], L.G. Gerling[a], C. Voz[a], C. del Cañizo[b], R. Alcubilla[a]

[a] Electronic Engineering Department, Universitat Politècnica de Catalunya, Jordi Girona 1-3, Barcelona 08034, Spain
[b] Instituto de Energía Solar, Universidad Politécnica de Madrid, 28040 Madrid, Spain

ARTICLE INFO

Keywords:
Germanium
MoOx
Transition metal oxide
Solar cell
Thermophotovoltaics
Photovoltaics

ABSTRACT

Very thin, thermally evaporated MoO_x ($x < 3$) layer has been used as transparent hole-selective contact on an n-type Germanium substrate to effectively demonstrate PV conversion capability. The fabricated MoO_x/Ge heterojunction PV cell shows a photocurrent density of 44.8 mA/cm^2 under AM1.5G illumination, which is comparable to that of conventional Ge PV cells. However, a low open-circuit voltage of 138 mV is obtained, which might be explained by the presence of tunnelling mechanisms through the MoO_x/Ge interface. To our knowledge, this is the first demonstration of a hole-selective contact made of transition metal oxide on an n-type semiconductor different from c-Si. Thus, this work may have important implications toward the development of new device architectures, such as novel low-cost Ge PV cells with possible applications in multijunction solar cells and thermophotovoltaics.

Historically, the driving force for the use of Ge in photovoltaic (PV) applications has been as a substrate for GaAs space solar cells (Miller and Harris, 1980), the main reason being the higher thermal conductivity and the possibility of manufacturing thinner and lighter wafers with Ge than with GaAs. Later on, Ge/GaAs tandem solar cells were pursued to enhance the conversion efficiency (Chand et al., 1986) by using the Ge bottom cell to convert the infrared part of the solar spectrum. This progress eventually derived in the development of the current standard technology for space solar cells that consists of triple junction Ge/GaAs/GaInP structures, with AM0 conversion efficiencies in the range of 28–30%. These cells have been also used in terrestrial applications within concentrated-PV (CPV) systems, where they reached AM1.5D conversion efficiencies of 41.6% (King et al., 2009), just below the current world-record for solar-to-electricity conversion efficiency of 46.0% (Dimroth et al., 2016). Apart from solar applications, Ge PV cells have been considered as a low-cost replacement for low band gap III-V semiconductors in thermophotovoltaic (TPV) converters, in which thermal radiation is directly converted into electricity by infrared sensitive PV devices (Bauer, 2011; Chubb, 2007). In this context, Ge TPV cells could be used in a broad range of applications such as waste heat recovery (Bauer et al., 2003), solar-thermal power (Ungaro et al., 2015; Lenert et al., 2014; Datas and Algora, 2013), space power (Datas and Martí, 2017), and energy storage (Datas et al., 2016), among many others.

Current state of the art of Ge PV cells consist of p-n junctions created by diffusion of dopants at high temperatures (Bitnar, 2003). For instance, p-n junctions in p-Ge have been created by diffusion of V-group atoms (typically P and As) during the first growing step of GaInP or GaAs nucleation layers within a Metal-Organic CVD (MOCVD) reactor at temperatures of ~650 °C (Fernandez et al., 2008; Fernández, 2010; Barrigón Montañés, 2014). Other groups have used the diffusion of Zn in n-Ge substrates within a LPE reactor (Khvostikov et al., 2002). In an effort to reduce manufacturing costs of standalone Ge PV cells, IMEC reported devices with p-n junctions created by spin-on diffusion of P on p-Ge by rapid thermal annealing at different temperatures (450–700 °C) (Posthuma et al., 2007; van der Heide, 2009; van der Heide et al., 2009) leading to the best reported 1-sun AM1.5G conversion efficiency for stand-alone Ge PV cells of 7.9% (van der Heide et al., 2009). Surface passivation has been accomplished by forming different kinds of heterojunctions on Ge surface, such as Ge/GaAs (Khvostikov et al., 2002) or Ge/GaInP (Fernandez et al., 2008; Fernández, 2010; Barrigón Montañés, 2014) by MOCVD or LPE (Khvostikov et al., 2002), or Ge/a-Si (Posthuma et al., 2007; van der Heide, 2009; van der Heide et al., 2009; Posthuma et al., 2005), Ge/SiNx (Nagashima et al., 2007) and Ge/a-Si_xC_{1-x} (Fernandez et al., 2008; Fernández, 2010; Weiss et al., 2018) by PECVD.

In order to further reduce the fabrication cost of Ge PV cells, it is desirable to eliminate the high temperature diffusion, and complex MOCVD or PECVD processes. In this regard, a particularly appealing option consists of substituting the doping step by carrier-selective coatings with surface passivation properties that could be deposited at low temperatures. For this purpose, high electron-affinity transition

* Corresponding authors.

https://doi.org/10.1016/j.solener.2019.02.009
Received 29 August 2018; Received in revised form 21 January 2019; Accepted 6 February 2019

metal oxides (TMOs) such as MoO_3, WO_3, and V_2O_5, are very interesting candidates that have already been found effective to produce hole-selective contacts on both n-type and p-type c-Si (Gerling et al., 2015; Battaglia et al., 2014; Bullock et al., 2014; Vijayan et al., 2018).

In this letter we report a Ge PV cell formed by a thin sub-stoichiometric MoO_x ($x < 3$) layer on top of an n-type crystalline Ge (c-Ge) substrate, which behaves as a hole selective contact. To our knowledge, this is the first demonstration of a hole-selective contact made with a TMO on an n-type semiconductor different than c-Si. Thus, it might open the door to new device architectures, not only for PV applications, but also in photonics and CMOS electronics, where the integration of TMOs is being investigated (Sanchez et al., 2016), along with the use of different semiconductors having higher carrier mobilities and extended spectral response than c-Si, such as Ge (Reboud et al., 2017; Toriumi and Nishimura, 2017).

The PV cell structure was fabricated on (1 0 0) oriented, Czochralski, n-type Ge substrates ($\rho = 0.37\ \Omega$·cm, 350 µm-thick). The substrate was cleaned by HCl: H_2O (33%) immediately prior to rear side passivation by PECVD of (i/n^+) a-SiC_x:H (4/15 nm, x ~ 0.2) and a-SiC (80 nm) stack deposited at ~300 °C. Next, the rear contact was created by laser firing of the a-SiC stack to produce an array of ~60 µm diameter local diffusion points, separated by 600 µm pitch. This distance was chosen to introduce reasonable series resistance of ~0.1 Ωcm^2 (Fischer, 2003). Laser firing was accomplished by means of a ~1200 mW, $\lambda = 1064$ nm Nd/YAG laser system at a frequency of 4 kHz with 6 pulses per spot, following a similar approach developed for c-Si devices (López et al., 2018). The rear contact was finalized by means of an e-beam evaporated Ti/Pd/Ag metal stack that provides lateral interconnection between fired points. The hole selective contact was formed at the front side of the device by means of very thin (nominally 20 nm) MoO_x layer thermally evaporated from powdered MoO_3 sources at ~$8{\cdot}10^{-6}$ mbar and a deposition rate of ~0.2 Å/s (Gerling et al., 2015). A 75 nm-thick ITO layer was subsequently deposited by RF-Sputtering on top of the MoO_x layer to increase lateral electrical conductivity and minimize optical reflectivity. A sketch of the full PV cell structure and the TEM image of the MoO_x/ITO interface are shown in Fig. 1, where a pronounced inter-diffusivity between the layers is clearly observed. The 1x1 cm^2 active area of the PV cells was defined by conventional lithographic techniques followed by mesa etching of the MoO_x/ITO layers. Finally, the front Ag grid electrode (2 µm thick) was evaporated through a shadow mask for a 4% contacted area.

One-sun *I-V* characterization of the PV cell was performed at 25 °C using a ORIEL 94021A (Newport) solar simulator, where the distance between the cell and the lamp was varied until the photo-generated current density coincides with the one calculated through the integration of the cell' experimental external quantum efficiency (EQE) and the AM1.5G spectrum with 100 mW/cm^2. The corresponding current density-voltage (*J-V*) curve under 1-sun illumination is shown in Fig. 2. The short-circuit current density (J_{SC} = 44.8 mA/cm^2) outperforms that of the best performing state of the art Ge PV cells (43.2 mA/cm^2) (van der Heide et al., 2009). On the other hand, a much lower open circuit voltage (138 mV) is measured, compared to those reported in (Fernández, 2010; van der Heide et al., 2009) (up to 265 mV), which ultimately results in a lower FF (40.9%), partially due to a non-optimized metal grid that introduces a series resistance of 0.65 Ωcm^2. As a result, an AM1.5G conversion efficiency of 2.53% is obtained.

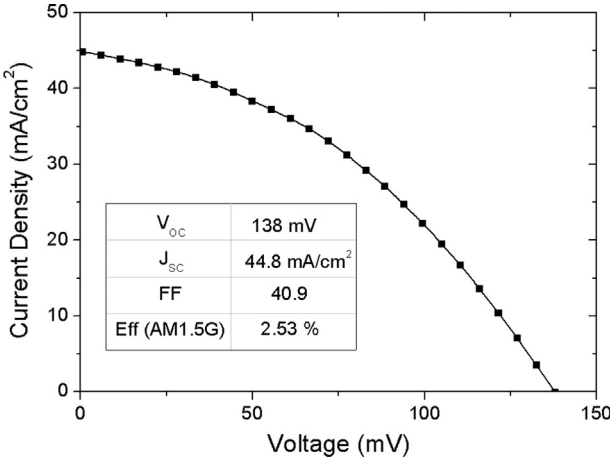

Fig. 2. Current density-voltage curve of the Ge PV cell manufactured in this work under AM1.5 G illumination conditions.

External quantum efficiency (EQE) of the PV cell is shown in Fig. 3 at short-circuit conditions along with the EQE of Ge PV cells reported in (van der Heide, 2009) for a direct comparison. The improved EQE for wavelengths shorter than 600 nm might be explained by the reduction of the recombination close to the front surface compared to the one existing in the highly-doped emitters (10^{19}–10^{21} cm^{-3}) used in (van der Heide, 2009). Such a low recombination does not necessary indicate a good chemical surface passivation, i.e. strong reduction of interface state density, but it could be related to a strong electric field that unbalances carrier densities, i.e. field-effect passivation. The electric field located at the surface creates an electrostatic potential which, under thermal equilibrium, is the potential barrier built at the junction (V_{bi}). Then, the higher V_{bi}, the stronger the electric field and, thus, the better the surface passivation. In order to measure V_{bi}, capacitance-voltage measurements of the cell in reverse bias were performed at 10 kHz using HP4294A impedance analyser with a signal amplitude of 30 mV following the same approach than in (Almora et al., 2017) where similar structures on c-Si substrates are characterized. This data can be

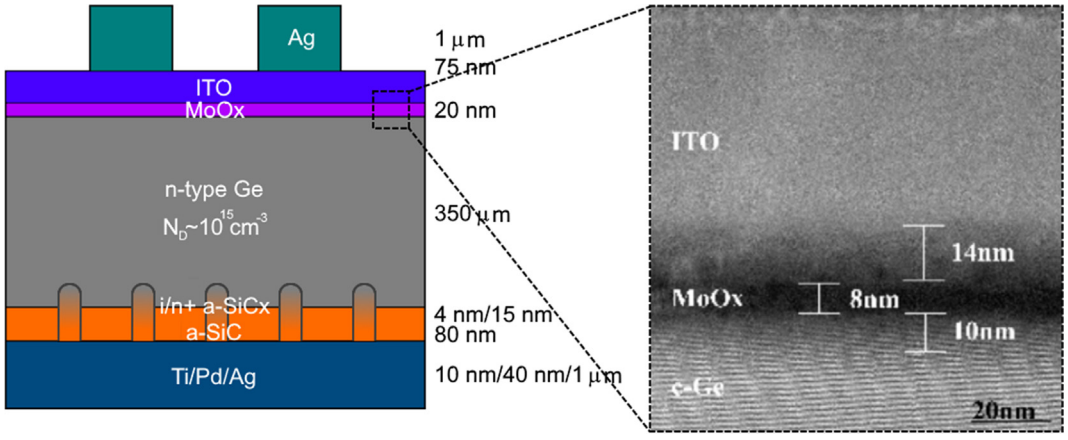

Fig. 1. Sketch of the fabricated solar cell. Focus: TEM image of the MoO_x interlayer of the final device.

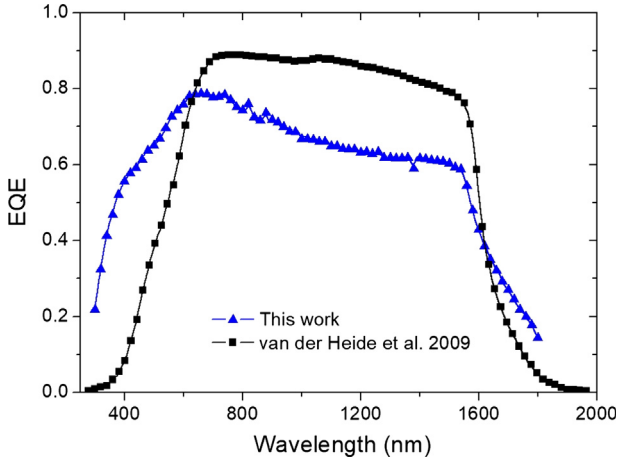

Fig. 3. External quantum efficiency of the Ge PV cell manufactured in this work along with that of the Ge PV cell reported in (van der Heide 2009).

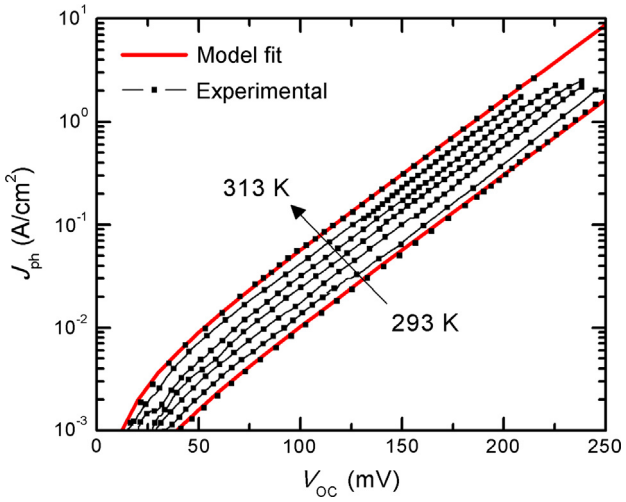

Fig. 4. J_{ph}-V_{OC} curves at different temperatures from 293 to 333 K in 5 K steps.

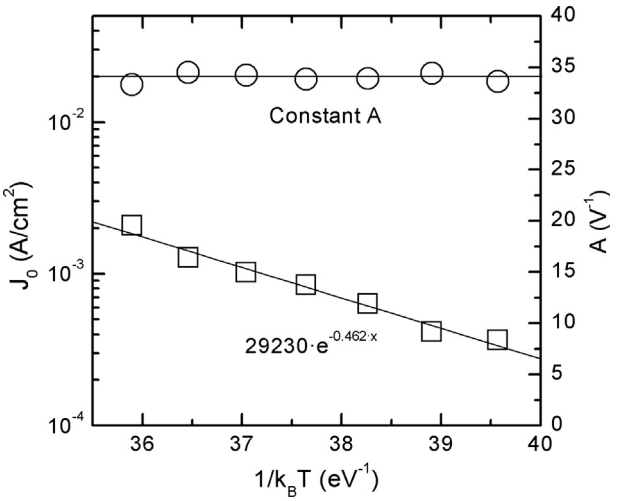

Fig. 5. Arrhenius plot of the saturation current density (J_0) and the prefactor of the exponent (A). Experimental data (symbols) are fit with theoretical expressions (lines) leading to the determination of a constant A with an activation energy of 0.462 eV. The constant A value with temperature suggests a tunnel current mechanism.

obtained by fitting the C^{-2} vs. V curve, known as Mott-Schottky plot, using the following equation $1/C^2 = 2(V_{bi} - V - 2k_BT/q)/q\varepsilon_S N_D$, where symbols have their usual meanings, i.e. k_B is the Boltzmann constant, T is the cell's temperature, q is the electron's charge, ε_S is the semiconductor electrical permittivity, and N_D is the doping level. By applying this model to the experimental data, we get an almost perfect linear fit ($R^2 = 0.99988$) leading to $V_{bi} = 317 \pm 4$ mV. Additionally, the doping density (N_D) can be obtained from the slope of the curves leading to a N_D value of $6.9 \pm 0.1 \cdot 10^{15}$ cm^{-3}, which fully agrees with the Ge substrate specifications. The calculated V_{bi} indicates that the surface is highly inverted, i.e. hole density at the surface is even higher than the doping density N_D, reducing interface recombination due to the scarce availability of electrons. This might explain the relatively high EQE values measured under short-circuit conditions in the UV–visible range. In Fig. 6, we show a tentative band diagram of the structure where the electron rejection due to the band bending in the c-Ge under thermal equilibrium is indicated.

In order to investigate the origin of the low V_{OC}, a further understanding of the current mechanisms taking place in the MoO_x/Ge heterojunction is needed. With this aim, open-circuit voltage (V_{OC}) is measured as a function of photogenerated current (J_{ph}) by means of a flash lamp, also known as Suns-*Voc* measurement. For every flash, V_{oc} values of the cell are recorded in an oscilloscope, while J_{ph} is estimated from the light intensity measured by a reference Ge PV cell (Kerr et al., 2001). It is well known that applying the superposition principle and taking into account that the device is kept under open-circuit conditions, J_{ph} must be equal to the current that would be measured in the cell at dark conditions and the series resistance has no effect on the measurement. As a consequence, the analysis of J_{ph}-V_{OC} curves enables the extraction of useful information otherwise hidden by the series resistance effects in conventional dark *J-V* characteristics. This advantage is crucial in our devices given the combination of relatively high currents with significant series resistance. Fig. 4 shows the J_{ph}-V_{oc} curves measured at temperatures ranging 293–323 K in 5 K steps. The experimental data are fitted to an exponential trend given by $J_{ph} = J_0(T)[\exp(A(T)\cdot V_{OC}) - 1]$ and two examples for the highest and lowest temperature measurement are also shown in Fig. 4. Notice that in this model no series resistance is included and consequently we have only two free parameters: the saturation current density, J_0(T), and the exponential factor, $A(T)$. In Fig. 5 we show the Arrhenius plot of these parameters where a constant value of $A \approx 34\ V^{-1}$ and an activation energy of 0.462 eV for $J_0(T)$ suggests that tunnelling mechanism dominates at the MoO_x/Ge interface (Sze and Ng, n.d.). In Fig. 6, we sketch a possible explanation for this tunnelling corresponding to electrons from the MoOx conduction band to the c-Ge valence band following the models reported in (Vijayan et al., 2018). This tunnelling current

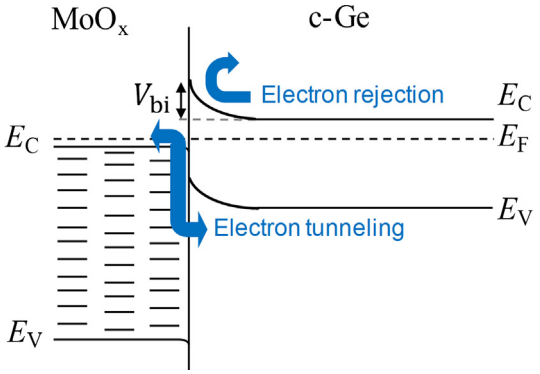

Fig. 6. Proposed band-diagram of the MoO_x/Ge heterostructure.

jeopardizes the electron blocking properties at the conduction band of the junction leading to a high saturation current density and, thus, low V_{oc} values. Despite the mechanism proposed hereby is a reasonable guess, a deeper knowledge of the band structure and interface characteristics of MoO_x/Ge junction is needed to fully understand how this

tunnel mechanism takes place and to improve the obtained V_{oc} values.

In conclusion, we have reported for the first time a heterojunction MoO_x/Ge PV cell that effectively demonstrates the possibility of creating hole selective contacts in n-type c-Ge. Photovoltaic performance of the device shows excellent J_{sc} values (44.8 mA/cm^2) mainly related to an enhanced spectral response at short wavelengths. On the other hand, low V_{oc} values (138 mV) might be explained by an excess of tunnel current at the MoO_x/Ge interface resulting in high saturation currents. With evident room for improvement, these results could eventually open a new route for cost-reduction of Ge-based PV devices, including the development of new kind of low cost thermophotovoltaic converters. Eventually, it could also open the door for the integration of transition metal oxides in Ge photonics and CMOS electronics.

Acknowledgements

This work was supported by MINECO (Ministerio de Economía y Competitividad de España) under Thin-IBC [TEC2017-82305-R], CHENOC [ENE2016-78933-C4-1-R], and TORMES [ENE2015-72843-EXP] projects, and by the EU project AMADEUS, which has received funds from the Horizon 2020 research and innovation program, FET-OPEN action, under grant agreement no. 737054. A.Datas acknowledges postdoctoral fellowship support from the Spanish “Juan de la Cierva-Incorporación” program (IJCI-2015-23747). The sole responsibility for the content of this publication lies with the authors. It does not necessarily reflect the opinion of the European Union. Neither the REA nor the European Commission are responsible for any use that may be made of the information contained therein.

References

Almora, Osbel, Gerling, Luis G., Voz, Cristóbal, Alcubilla, Ramón, Puigdollers, Joaquim, Garcia-Belmonte, Germà, 2017. Superior performance of V_2O_5 as hole selective contact over other transition metal oxides in silicon heterojunction solar cells. Solar Energy Mater. Solar Cells 168 (August), 221–226. https://doi.org/10.1016/j.solmat.2017.04.042.

Barrigón Montañés, Enrique, 2014. Development of GaInP/GaInAs/Ge TRIPLE-Junction Solar Cells for CPV Applications. Phd. E.T.S.I. Telecomunicación (UPM). http://oa.upm.es/30449/.

Battaglia, Corsin, Yin, Xingtian, Zheng, Maxwell, Sharp, Ian D., Chen, Teresa, McDonnell, Stephen, Azcatl, Angelica, et al., 2014. Hole selective MoOx contact for silicon solar cells. Nano Lett. 14 (2), 967–971. https://doi.org/10.1021/nl404389u.

Bauer, T., 2011. Thermophotovoltaics: basic principles and critical aspects of system design. Green Energy and Technology. Springer.

Bauer, T., Forbes, I., Penlington, R., Pearsall, N., 2003. The potential of thermophotovoltaic heat recovery for the glass industry. 653 In: Coutts Timothy, J., Guido, Guazzoni, Joachim, Luther (Eds.), AIP, pp. 101–110.

Bitnar, Bernd, 2003. Silicon, germanium and silicon/germanium photocells for thermophotovoltaics applications. Semicond. Sci. Technol. 18 (5), S221. https://doi.org/10.1088/0268-1242/18/5/312.

Bullock, James, Cuevas, Andres, Allen, Thomas, Battaglia, Corsin, 2014. Molybdenum oxide MoOx: a versatile hole contact for silicon solar cells. Appl. Phys. Lett. 105 (23), 232109. https://doi.org/10.1063/1.4903467.

Chand, N., Klem, J., Henderson, T., Morkoç, H., 1986. Diffusion of As and Ge during growth of GaAs on Ge substrate by molecular-beam epitaxy: its effect on the device electrical characteristics. J. Appl. Phys. 59 (10), 3601–3604. https://doi.org/10.1063/1.336790.

Chubb, D.L., 2007. Fundamentals of thermophotovoltaic energy conversion. Elsevier.

Datas, Alejandro, Algora, Carlos, 2013. Development and experimental evaluation of a complete solar thermophotovoltaic system. Progr. Photovolt.: Res. App. 21 (5), 1025–1039. https://doi.org/10.1002/pip.2201.

Datas, A., Martí, A., 2017. Thermophotovoltaic energy in space applications: review and future potential. Solar Energy Mater. Solar Cells 161 (March), 285–296. https://doi.org/10.1016/j.solmat.2016.12.007.

Datas, Alejandro, Ramos, Alba, Martí, Antonio, del Cañizo, Carlos, Luque, Antonio, 2016. Ultra high temperature latent heat energy storage and thermophotovoltaic energy conversion. Energy 107 (July), 542–549. https://doi.org/10.1016/j.energy.2016.04.048.

Dimroth, F., Tibbits, T.N.D., Niemeyer, M., Predan, F., Beutel, P., Karcher, C., Oliva, E., et al., 2016. Four-junction wafer-bonded concentrator solar cells. IEEE J. Photovolt. 6 (1), 343–349. https://doi.org/10.1109/JPHOTOV.2015.2501729.

Fernández, J., 2010. Optimization of crystalline germanium for thermophotovoltaic and high-efficiency solar cells. University Konstanz.

Fernandez, J., Janz, S., Suwito, D., Oliva, E., Dimroth, F., 2008. Advanced concepts for high-efficiency germanium photovoltaic cells. In: In 2008 33rd IEEE Photovoltaic Specialists Conference, pp. 1–4. https://doi.org/10.1109/PVSC.2008.4922631.

Fischer, Bernhard, 2003. Loss analysis of crystalline silicon solar cells using photoconductance and quantum efficiency measurements. Cuvillier, Gottingen.

Gerling, Luis G., Mahato, Somnath, Morales-Vilches, Anna, Masmitja, Gerard, Ortega, Pablo, Voz, Cristobal, Alcubilla, Ramon, Puigdollers, Joaquim, 2016. Transition metal oxides as hole-selective contacts in silicon heterojunctions solar cells. In: Solar Energy Materials and Solar Cells 145. pp. 109–115. https://doi.org/10.1016/j.solmat.2015.08.028.

Kerr, Mark J., Cuevas, Andres, Sinton, Ronald A., 2001. Generalized analysis of quasi-steady-state and transient decay open circuit voltage measurements. J. Appl. Phys. 91 (1), 399–404. https://doi.org/10.1063/1.1416134.

Khvostikov, V.P., Khostikov, O.A., Oliva, E.V., Rumyantsev, V.D., Shvarts, M.Z., Tabarov, T.S., Andreev, V.M., 2002. Zinc-diffused InAsSbP/InAs and Ge TPV Cells. In: Conference Record of the Twenty-Ninth IEEE Photovoltaic Specialists Conference, pp. 943–946. https://doi.org/10.1109/PVSC.2002.1190736. 2002.

King, R.R., Boca, A., Hong, W., Liu, X.-Q., Bhusari, D., Larrabee, D., Edmondson, K.M., Law, D.C., Fetzer, C.M., Mesropian, S., Karam, N.H., 2009. Band-gap-engineered architectures for high-efficiency multijunction concentrator solar cells. In: 24th European Photovoltaic Solar Energy Conference and Exhibition, Hamburg, Germany, https://doi.org/10.4229/24thEUPVSEC2009-1AO.5.2.

Lenert, Andrej, Bierman, David M., Nam, Youngsuk, Chan, Walker R., Celanovic, Ivan, Soljacic, Marin, Wang, Evelyn N., 2014. A nanophotonic solar thermophotovoltaic device. Nat Nano 9 (2), 126–130.

López, G., Jin, C., Martín, I., Alcubilla, R., 2018. Impact of C-Si surface passivating layer thickness on n^+; laser-doped contacts based on silicon carbide films. IEEE J. Photovolt. 8 (4), 976–981. https://doi.org/10.1109/JPHOTOV.2018.2836963.

Miller, D.L., Harris, J.S., 1980. Molecular beam epitaxial GaAs heteroface solar cell grown on Ge. Appl. Phys. Lett. 37 (12), 1104–1106. https://doi.org/10.1063/1.91889.

Nagashima, Tomonori, Okumura, Kenichi, Yamaguchi, Masafumi, 2007. A germanium back contact type thermophotovoltaic cell. AIP Conf. Proc. 890 (1), 174–181. https://doi.org/10.1063/1.2711734.

Posthuma, N.E., Flamand, G., Geens, W., Poortmans, J., 2005. Surface passivation for germanium photovoltaic cells. Solar Energy Mater. Solar Cells 88 (1), 37–45. https://doi.org/10.1016/j.solmat.2004.10.005.

Posthuma, N.E., van der Heide, J., Flamand, G., Poortmans, J., 2007. Emitter formation and contact realization by diffusion for germanium photovoltaic devices. IEEE Trans. Electron Dev. 54 (5), 1210–1215. https://doi.org/10.1109/TED.2007.894610.

Reboud, V., Gassenq, A., Hartmann, J.M., Widiez, J., Virot, L., Aubin, J., Guilloy, K., et al., 2017. Germanium based photonic components toward a full silicon/germanium photonic platform. Progr. Crystal Growth Character. Mater. 63 (2), 1–24. https://doi.org/10.1016/j.pcrysgrow.2017.04.004.

Sanchez, L., Lechago, S., Gutierrez, A., Sanchis, P., 2016. Analysis and design optimization of a hybrid VO2/Silicon 2 x 2 microring switch. IEEE Photon. J. 8 (2), 1–9. https://doi.org/10.1109/JPHOT.2016.2551463.

Sze, S.M., Ng, K.K., 2016Sze and Ng, n.d.. Physics of semiconductor devices, 3ed ed. John Wiley & Sons.

Toriumi, Akira, Nishimura, Tomonori, 2017. Germanium CMOS potential from material and process perspectives: Be more positive about germanium. Japan. J. Appl. Phys. 57 (1), 010101. https://doi.org/10.7567/JJAP.57.010101.

Ungaro, Craig, Gray, Stephen K., Gupta, Mool C., 2015. Solar thermophotovoltaic system using nanostructures. Opt. Expr. 23 (19), A1149. https://doi.org/10.1364/OE.23.0A1149.

van der Heide, J., 2009. Cost-efficient thermophotovoltaic cells based on germanium. Katholieke Universiteit Leuven.

van der Heide, J., Posthuma, N.E., Flamand, G., Geens, W., Poortmans, J., 2009. Cost-efficient thermophotovoltaic cells based on germanium substrates. Solar Energy Mater. Solar Cells 93 (10), 1810–1816. https://doi.org/10.1016/j.solmat.2009.06.017.

Vijayan, R.A., Essig, S., De Wolf, S., Ramanathan, B.G., Löper, P., Ballif, C., Varadharajaperumal, M., 2018. Hole-collection mechanism in passivating metal-oxide contacts on si solar cells: insights from numerical simulations. IEEE J. Photovolt. 8 (2), 473–482. https://doi.org/10.1109/JPHOTOV.2018.2796131.

Weiss, C., Schön, J., Höhn, O., Mohr, C., Kurstjens, R., Boizot, B., Janz, S., 2018. Potential analysis of a rear-side passivation for multi-junction space solar cells based on germanium substrates. 45th IEEE Photovoltaic Specialists Conference. Hawaii, USA.